Atmospheric Environment 137 (2016) 80–89

Contents lists available at ScienceDirect

Atmospheric Environment

journal homepage: www.elsevier.com/locate/atmosenv

Reduced-form modeling of public health impacts of inorganic $PM_{2.5}$ and precursor emissions

Jinhyok Heo [a, *], Peter J. Adams [a, b], H. Oliver Gao [c]

[a] Department of Engineering and Public Policy, Carnegie Mellon University, Pittsburgh, PA 15213, USA
[b] Department of Civil and Environmental Engineering, Carnegie Mellon University, Pittsburgh, PA 15213, USA
[c] School of Civil and Environmental Engineering, Cornell University, Ithaca, NY 14853, USA

HIGHLIGHTS

- Method brings results from detailed chemical transport models to policy analysis.
- Method estimates marginal social cost and intake fraction accurately and quickly.
- Reduced-form models produce errors comparable to state-of-the-art models' errors.

GRAPHICAL ABSTRACT

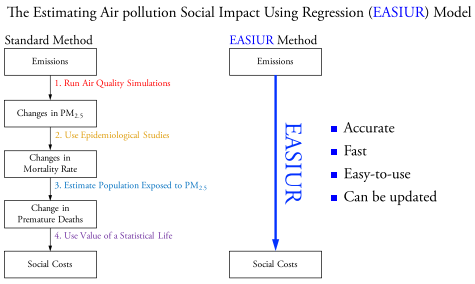

ARTICLE INFO

Article history:
Received 28 October 2015
Received in revised form
19 April 2016
Accepted 20 April 2016
Available online 22 April 2016

Keywords:
Marginal social costs
Intake fraction
$PM_{2.5}$
Public health
Air quality
Risk analysis
Chemical transport model
CAMx

ABSTRACT

It is challenging to estimate the public health costs of fine particulate matter ($PM_{2.5}$) and its precursor emissions accurately and quickly for policy research because of their complex physical and chemical processes occurring over a large downwind area. We developed a method for building statistical regressions that estimate public health cost of emissions accurately like a state-of-the-art chemical transport model (CTM) but without its high computational cost. This method achieves detailed spatial resolution according to the location of the emission source, accounting for differences in the exposed population downwind. Using tagged CTM simulations, our method builds a large dataset of air quality public health costs from marginal emissions throughout the United States. Two methods were developed to describe exposed population, one that assumes a generic downwind plume concentration profile derived from CTM outputs and a simpler method that uses the size of population within certain distances as variables. Using the former method, we parameterized marginal public health cost [$/t] and intake fraction [ppm] as a function of exposed population and key atmospheric variables. We derived models for elemental carbon, sulfur dioxide, nitrogen oxides, and ammonia. Compared to estimates calculated directly using CTM outputs, our models generally show mean fractional errors of only 10%–30% and up to 50% for NO_x in some seasons, which are generally similar to or less than CTM's performance. Our results show that the public health costs of emissions can be efficiently parameterized for policy analyses based on state-of-the-art CTMs.

1. Introduction

Accurate estimation of the impact of air pollutant emissions on society is valuable in several decision making arenas. Human

* Corresponding author. Current address: School of Civil and Environmental Engineering, Cornell University, Ithaca, NY 14853, USA.
E-mail address: jinhyokh@alumni.cmu.edu (J. Heo).

http://dx.doi.org/10.1016/j.atmosenv.2016.04.026
1352-2310/

activities such as generating electricity, heating and cooling, and transportation emit air pollutants, imposing undesirable burdens on humans and the natural environment. Strongly associated with cardiovascular and cardiopulmonary premature mortality (Pope and Dockery, 2006), fine particulate matter ($PM_{2.5}$) imposes serious public health burdens. In 2010, ambient particulate matter pollution was the 9th leading contributor (3.2 M–3.3 M premature deaths/year) to the global burden of disease (Lelieveld et al., 2015; Lim et al., 2012) and the 8th (103 k premature deaths/year) in the United States (US Burden of Disease Collaborators, 2013). Ambient $PM_{2.5}$ consists partly of primary (directly emitted) species, but mostly of secondary (chemically produced from gaseous precursors) species. Therefore, accurate estimation of air quality impacts must account for atmospheric chemical processing, which depends on meteorological conditions and frequently exhibits nonlinear behaviors. The major precursors for secondary $PM_{2.5}$ include sulfur dioxides (SO_2), nitrogen oxides (NO_x), ammonia (NH_3), and volatile organic compounds (VOCs).

A common way of quantifying the societal impacts of air pollution is based on an impact pathway analysis that converts air pollutant emissions to ambient concentrations, estimates their societal effects (e.g. premature mortality and other health effects), and monetizes these outcomes using estimates of willingness-to-pay to avoid these effects. It is a standard method used by the U.S. EPA in benefit-cost analyses of the Clean Air Act (U.S. EPA, 2011a, 1999) and other regulatory impact analyses. According to analyses based on this method (U.S. EPA, 2011a, 1999; National Research Council, 2010), premature mortality associated with $PM_{2.5}$ accounts for more than 90% of the monetized damages of air quality on public health and the environment. Therefore, policy analyses often focus on the mortality effects of $PM_{2.5}$.

A convenient measure to estimate the social cost of emissions is marginal social cost, which is public health cost caused by "marginal," or relatively small, amount of emissions, or marginal social benefit in case of marginal emission reductions. For inert primary $PM_{2.5}$ species, marginal benefit and marginal cost would have the same magnitude and public health cost is expected to be proportional to the amount of increased emissions when the characteristics of population exposure and meteorology are held constant. For secondary species with nonlinear behaviors, marginal effects may differ depending on whether emissions increase or decrease or whether baseline emissions of related species change. However, there would be a certain range of marginal emissions where marginal effects stay similar. For policy interventions that result in such marginal changes, their social cost can be easily calculated by multiplying marginal social cost by the change in emissions.

Intake fraction is a similar measure widely used to quantify the public health effects of emissions (Bennett et al., 2002). For atmospheric emissions, intake fraction is defined as the fraction of emissions that are inhaled by an exposed population. Compared to social cost, intake fraction focuses on characterizing the relationship of emissions to population exposure.

Policy research often requires quickly comparing many different policy options and exploring associated uncertainties. Current air quality tools face significant limitations in achieving this goal. Current tools may be divided into three categories. First, chemical transport models (CTMs) such as CAMx (ENVIRON, 2012) and CMAQ (Byun and Schere, 2006) are the most rigorous tools for simulating air quality. CTMs divide the atmosphere into a three-dimensional grid and attempt to simulate all the relevant processes of pollutant transport, chemical reaction, and removal of particles and gases in the atmosphere. Because CTMs are computationally expensive, several CTM add-ons were developed to enhance computational efficiency such as Particulate Source Apportionment Technology (PSAT) (Koo et al., 2009; Kwok et al., 2015; Wagstrom et al., 2008), Direct Decoupled Method (DDM) (Dunker et al., 2002; Koo et al., 2007), and Adjoint (Hakami et al., 2007; Henze et al., 2007). PSAT puts tags on emission sources to track their contributions at multiple receptor locations. DDM allows to find sensitivity of emission sources and parameters to results at multiple receptors. Conversely, Adjoint method calculates sensitivity of changes in receptors to sources and parameters. However, being still computationally demanding, these sensitivity techniques may reduce CTM's computational burden one or two orders of magnitude but not more than that. Because running CTMs with or without such an add-on are computationally expensive, they are often employed for a limited number of scenarios even for important regulatory impact analyses.

Second, tools such as COBRA (U.S. EPA, 2013) and APEEP/AP2 (Muller, 2011; Muller and Mendelsohn, 2009) estimate social costs for all (~3000) U.S. counties using the Climatological Regional Dispersion Model (CRDM) (Latimer, 1996), which a CTM would require roughly 6000 CPU-years to generate according to our back-of-envelop calculation. However, Gaussian dispersion models such as CRDM have fundamental limitations. They assume that meteorological conditions at the source are held constant for all downwind areas, posing potential problems in predicting secondary $PM_{2.5}$ formations. These dispersion-based models have at best simple treatments of inorganic $PM_{2.5}$ formation chemistry and rely on an outdated understanding of organic $PM_{2.5}$ formation from volatile organic compounds, which has substantially revised in recent years (Robinson et al., 2007).

Lastly, there are per-ton social costs estimated by a statistical model built using CTM outputs (Fann et al., 2009; U.S. EPA, 2006) and by directly using CTM simulations (Fann et al., 2012; U.S. EPA, 2014). However, due to their CTM's high computational costs, their estimates are limited to certain urban areas and/or national averages for a selected set of sectoral emissions. Therefore, they do not provide a high spatial resolution according to emissions source, which is frequently useful in policy research. In short, because of current tools' limitations, a large part of policy research community is not able to incorporate the latest atmospheric science into their work.

In this paper, we present a new method called Estimating Air pollution Social Impacts Using Regression (EASIUR). The goal of the EASIUR method is to overcome the limitations noted above by deriving parameterizations that estimate marginal social costs [$/t] and intake fractions [ppm] from a large dataset of tagged simulations created by a CTM. The parameterizations provide a high spatial resolution similar to the county scale of CRDM and their outcomes produced with negligible computational costs are very similar to CTM-based estimates. As a proof of concept, we present the method and evaluation of the EASIUR model for one primary $PM_{2.5}$ species (elemental carbon) and three secondary inorganic $PM_{2.5}$ precursor species (sulfur dioxide, nitrogen oxides, and ammonia) for four seasons and for three emission heights: ground-level area emissions and two stack-height (150 m and 300 m) point sources. This paper focuses mainly on marginal social cost and most equivalent parts associated with intake fraction are included in the Supporting Information (SI). Challenges that are addressed in this study include finding methods to estimate downwind exposed populations, assessing the length of CTM simulations required, and finding methods that account for seasonal and other differences in atmospheric processing. EASIUR model's estimates and associated uncertainties are presented and discussed comprehensively in a separate study (Heo et al., 2016).

2. Method

2.1. Overview

The EASIUR method addressed technical challenges of computationally efficient but precise atmospheric modeling in several ways. First, for up-to-date atmospheric modeling, we employ a state-of-the-art CTM to estimate air quality changes, social costs, and intake fractions from marginal emissions at 100 randomly selected locations in the United States. Second, to reduce the computational costs of these simulations, we employed a tagged simulation technique and looked at the simulation period required to represent a season. Third, for quantifying dilution and population exposure occurring over a large downwind (hundreds of kilometers or more) area, we developed two methods. Lastly, we derived regression models that parameterize marginal social costs and intake fractions using exposed population metrics and atmospheric variables. We validated the model performance with out-of-sample tests. In the following, we described the details of model development.

2.2. Tagged air quality simulation with a chemical transport model

To predict $PM_{2.5}$ formation and impacts, we ran a regional-scale chemical transport model, the Comprehensive Air Quality Model with extensions (CAMx) (ENVIRON, 2012) using inputs developed for a major regulatory impact analysis (U.S. EPA, 2011b). CAMx simulates the formation, chemical transformation, transport and removal processes of primary and secondary $PM_{2.5}$ and their precursors (ENVIRON, 2012). The modeling platform has been comprehensively evaluated and showed good performance for estimating the $PM_{2.5}$ concentrations associated with elemental carbon, sulfur dioxides, nitrogen oxides, and ammonia, which are the species of our interest in this study (U.S. EPA, 2011c).

The model domain covers the contiguous United States and adjacent portions of Mexico and Canada with a horizontal grid resolution of 36 km × 36 km and 14 vertical layers reaching 16 km high. Due to long transport nature of $PM_{2.5}$ and precursors, the 36 km resolution may have small (~10%) biases compared to finer resolutions such as 12 km and 4 km (Arunachalam et al., 2011; Punger and West, 2013; Thompson et al., 2014). The emission inventory (U.S. EPA, 2011d) was created for year 2005 and includes emissions from Mexico and Canada. Meteorological input data for 2005 were generated by MM5 (Grell et al., 1994). The initial and boundary conditions were generated by GEOS-Chem, a global-scale chemical transport model (http://acmg.seas.harvard.edu/geos/).

The Particulate Matter Source Apportionment Technology (PSAT) (Koo et al., 2009; Wagstrom et al., 2008), a CAMx module, played an important role in generating our dataset efficiently. With PSAT, we simulated the changes in $PM_{2.5}$ concentrations from marginal air pollutant emissions by tagging emissions from 50 different locations in a single CAMx run. PSAT reduced computational time and disk space by a factor of 10 compared to the brute-force method of separate CAMx simulations for each marginal emissions perturbation. Although PSAT does not address indirect effects by design (e.g. more atmospheric oxidants from reducing NO_x may increase more sulfate $PM_{2.5}$ formation) (Koo et al., 2009), our PSAT setup takes indirect effects into account at least for the size of perturbations we chose because we compare two sets of PSAT simulations, one with baseline emissions and the other with perturbed emissions, and our sensitivity simulations show that potential biases from indirect effects are small over a wide range of perturbations, as will be described more below.

2.3. Marginal social cost

We used a standard impact pathway method to calculate the per-tonne social costs. Once a CTM calculates the changes in $PM_{2.5}$ concentrations on annual average ($\Delta c_{x,y}$ in $\mu g/m^3$) at each grid cell (x, y) of the simulation domain from given emissions, the changes in mortality ($\Delta y_{x,y}$ in number of premature deaths) at each downwind location are estimated by a health-impact function, Eq. (1) (Hubbell et al., 2005; U.S. EPA, 2015a):

$$\Delta y_{x,y} = y^0_{x,y} \cdot \left\{ 1 - \exp\left(-\frac{\ln R}{10} \cdot \Delta c_{x,y} \right) \right\} \quad (1)$$

where $y^0_{x,y}$ is the baseline mortality at (x, y), or the product of the baseline mortality rate and the population at (x, y), and R is the relative risk reported by epidemiological studies, that is, the changes in mortality rate over an increase of 10 $\mu g/m^3$ in $PM_{2.5}$ concentrations. U.S. EPA usually uses two relative risks, 1.06 from Krewski et al. (2009) and 1.14 from Lepeule et al. (2012), due to pros and cons of cohorts of the two studies (Krewski et al., 2003; U.S. EPA, 2011a). Among the two, we chose 1.06 for our modeling. However, we by no means endorse this value over the other. To make our method flexible, we provide an easy method in SI to adjust our results over a reasonable range of relative risk.

The next step is to valuate the changed mortality using Value of a Statistical Life (VSL in $). The per-tonne social cost (S in $/t) is calculated as follows:

$$S = \frac{\sum_{x,y} \Delta y_{x,y} \cdot \mathrm{VSL}}{E} \quad (2)$$

where E is the amount of annual emissions (in metric ton). We used $8.6 million in 2010 USD for VSL, which is a U.S. EPA-recommended value adjusted for 2005 income level. We show how to adjust our estimates for dollar year and income level and discuss timing of premature death after exposure to $PM_{2.5}$ in SI. Intake fraction is defined in SI.

2.4. Building a dataset

We built a dataset of marginal social costs and intake fractions using tagged CAMx simulations. The procedure is illustrated in Fig. 1 using a case for elemental carbon in summer. The two metrics were calculated using a size of marginal emissions, which is chosen after exploring a wide range.

First, we selected two sets of 50 CAMx source cells randomly based on the population in the CAMx grid. One set was used for building regression models and the other is held out for out-of-sample evaluation. Since social costs are largely determined by the number of people exposed in the surrounding region, we covered different population sizes by selecting five locations randomly at every 10th percentile by population size among non-zero population cells to select 50 locations per set. The same location was not selected for both sets. We used population in 2005 prepared for the CAMx grid using PopGrid version 4.3 and BenMAP Community Edition version 1.1 (both available at http://www2.epa.gov/benmap). To match the cohort age of the chosen concentration-response relation, we used only adult population of age 30 or older. In SI, we presented how to adjust our estimates for population and mortality rate in a different year.

Second, CAMx PSAT was run for a base case and marginal emission cases for the entire year of 2005. The marginal cases were run by adding a carefully chosen amount of emissions for each species in addition to the baseline 2005 emissions inventory. Above a certain size of emissions, the $PM_{2.5}$ increase per emissions may

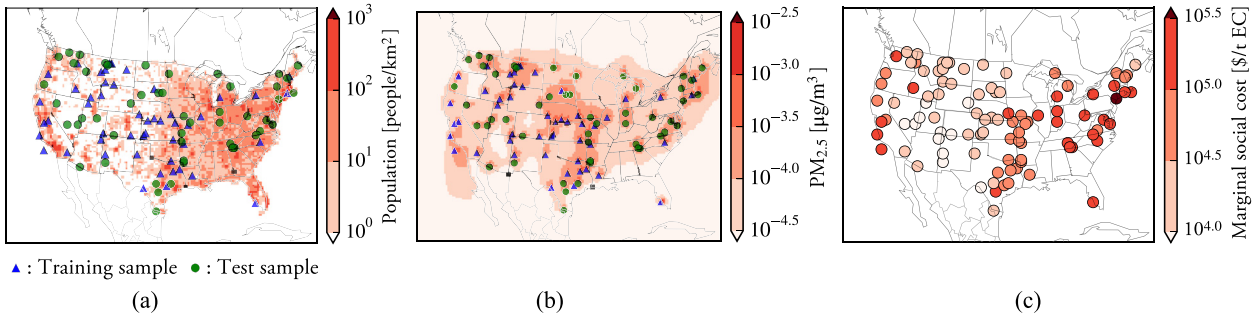

Fig. 1. Three steps of building a dataset for parameterization. For (b) and (c), the case of elemental carbon in summer is shown for illustration. (a) Two sample sets of 50 locations (one set for building models and the other for testing) were created randomly based on population size in the CAMx grid. (b) Distributions of $PM_{2.5}$ concentration created by marginal emissions for all sample locations (shown here together to illustrate) were produced from tagged CTM simulations. (c) Marginal social costs (shown here) and intake fractions were calculated using a standard impact pathway method for each location.

change due to nonlinearities in the chemistry (Ansari and Pandis, 1998) and, as a result, estimated marginal effects may not be valid anymore. Conversely, if the size of additional emissions is too small for the numerical precision of CAMx, model results may become unreliable due to numerical round-off noise.

In order to determine a proper size for a marginal emissions perturbation, we calculated social costs over a wide range of perturbed emissions. We ran CAMx PSAT simulations with ground-level emissions of $\overline{E} \times 4^{k}$ ($k = -4,\ldots, 1$) added at each training sample. $\overline{E}$ is the annual-average emissions (of both area and point sources) among non-zero emission cells in the CAMx grid. Then, we ran each simulation for January and July, the two most meteorologically contrasting months. After analyzing the results, we chose $\overline{E} \times 4^{-2}$ as the size of marginal emissions in our modeling (EC: 6.6 kg/cell/day, SO_2: 190 kg/cell/day, NO_x: 270 kg/cell/day, and NH_3: 69 kg/cell/day), which corresponds to an emissions increase by 6.25% of the per-cell annual-average emissions. Sensitivity to this value is analyzed below in Section 3.1. Then, CAMx was run for the marginal emission cases at the ground level for the entire year for both training and testing sample sets. Here we define winter from January to March, spring from April to June, summer from July to September, and fall from October to December. Considering the stack height distribution of current power plants, which goes up to 370 m high, we additionally ran marginal cases for two stack heights: 150 m and 300 m. For elevated emissions, we ran simulations only for the 50 training locations and did validations differently (Section 2.5.3). We simulated additional 10 days prior to all our simulations but did not include in the analysis to prevent results from being distorted from initial conditions.

Finally, the changes in $PM_{2.5}$ concentrations from marginal emissions against the base case were calculated for all sample locations. While we calculated the changes for inert EC using EC concentration outputs only, we used all $PM_{2.5}$ species for three inorganic pollutants (SO_2, NO_x, and NH_3), which will take into account relevant chemical reactions associated with the marginal addition of each inorganic pollutant. Then, marginal social costs and intake fractions were calculated for each location for each season as described in Section 2.3.

2.5. Model derivation

2.5.1. Regression approach

Because most variables are highly skewed as shown in Figs. S3–S6, the EASIUR models were fit with a log-log functional form as follows:

$$\ln S = \alpha + \beta \cdot \ln P + \sum_i \gamma_i \cdot \ln A_i + \varepsilon, \quad i = 1, \ldots, k \tag{3}$$

where S is the per-tonne social cost [$/t] or intake fraction [ppm], P is the exposed population (described in Section 2.5.2), and A_i's are atmospheric variables. The α, β, and γ_i parameters are regression coefficients and ε is the error term. For A_i, we tried several variables from the MM5 meteorological fields: temperature [K], surface atmospheric pressure [hPa], wind speed [m/s], absolute humidity [ppm], precipitation water content [g/m^3], cloud optical depth (dimensionless), and vertical diffusivity [m^2/s]. We used seasonal average values for all atmospheric variables.

To capture the nonlinear interactions between SO_2, NO_x, and NH_3 (Ansari and Pandis, 1998; West et al., 1999), we additionally tried the following atmospheric parameters: total sulfate ($TS \equiv SO_4^{2-}$ [mol/m^3]), total nitrate ($TN \equiv HNO_3 + NO_3^-$ [mol/m^3]), total ammonia ($TN \equiv HNO_3 + NO_3^-$ [mol/m^3]), free ammonia ($FA \equiv TA - 2 \cdot TS$ [mol/m^3]), the gas ratio (Ansari and Pandis, 1998), and the adjusted gas ratio (Pinder et al., 2008). In this context, "total" refers to the sum of concentrations in both gas and particle phases.

We fitted Eq. (3) with the training sample dataset for all possible combinations of explanatory variables. We used the Akaike information criterion (AIC) to select the best models, which favors the goodness of fit but also penalizes for the number of parameters to discourage overfitting (Akaike, 1974).

2.5.2. Methods of describing population exposure

It is crucial and challenging to parameterize in an efficient way the population exposed to $PM_{2.5}$ from marginal emissions. In general, population near an emission source is exposed to higher concentrations of air pollutants than those far from the source. However, despite lower concentrations, the potential size of exposed population may be much larger in areas far from the source, and $PM_{2.5}$ as its precursors can be transported hundreds of kilometers. Because different species undergo different atmospheric chemical processes, the magnitude and extent of their impacts are different, which makes it more complicated to characterize the population exposure. Therefore, a successful approach for dealing with this should weight population nearer a source more heavily and to address different species differently.

We tried to accomplish this goal of describing the varying population exposure around an emission source with two methods: "average plume" and "population ring" methods. As we found that the average plume method works better than the other, we built our final models with the average plume method.

The average plume describes the spatial distribution of $PM_{2.5}$ impacts around an emissions source, accounting for transport, dispersion, chemical conversion, and removal in the downwind region. The average plumes are generic downwind concentration profile derived from CTM simulations in order to assess population exposure. To generate an average plume, the spatial distribution of $PM_{2.5}$ impacts for all 50 training samples were: 1) translated in space so that they all had their emissions sources at a common origin location; 2) rotated so that the prevailing wind directions were in the same direction; 3) normalized so that the $PM_{2.5}$ concentrations summed across all grid cells is one. After these procedures, the 50 plumes were averaged to obtain a generic spatial distribution of $PM_{2.5}$ impacts, which we refer to as an "average plume," and indicate the fraction of the total $PM_{2.5}$ impact to be expected at downwind grid cells. A separate average plume is generated for each species emitted and season of the year. A weighted population, P in Eq. (3), is calculated by placing an average plume at a source location of interest and aligning the plume according to the dominant wind direction. The exposed population, P, is the sum of populations in each grid cell weighted by the average plume.

The other method is the "population ring" method. It uses the population within a certain distance from an emission source as a variable representing exposed population similarly as tried in some studies (Buonocore et al., 2014; Levy et al., 2009). This method is more described in SI.

2.5.3. Model evaluation

For the chosen regression models, we evaluated the ground-level emission models with the 50 test samples and the elevated emission models with a five-fold cross-validation method. The five-fold procedure randomly divided the 50 samples into five groups or "folds." Regression models were built using four groups and validated with the remaining group. It was then repeated five times with each group as a validation fold.

We adopted the model performance criteria suggested by Morris et al. (2005), which is commonly used to evaluate prediction of chemical transport models against measurement. The criteria are based on mean fractional bias and mean fractional error:

$$\text{Mean fractional bias} = \frac{2}{N}\sum_{i}^{N}\frac{P_i - O_i}{P_i + O_i} \quad (4)$$

$$\text{Mean fractional error} = \frac{2}{N}\sum_{i}^{N}\left|\frac{P_i - O_i}{P_i + O_i}\right| \quad (5)$$

where P_i is the EASIUR prediction from Eq. (4) above, O_i is the "true" estimate directly computed with CAMx outputs, and N is the number of test samples. Performance is considered "excellent" for fractional bias $\leq \pm 0.15$ and fractional error ≤ 0.35, "good" for fractional bias $\leq \pm 0.3$ and fractional error ≤ 0.5.

3. Results and discussion

3.1. Size of marginal emissions

We found that per-tonne social costs are insensitive to the size of perturbation over most of the wide range we tested, shown in Fig. S1. Marginal social costs of EC did not change much for the entire range we tested, which is expected because EC is inert. For SO_2, NO_x, and NH_3, they did not change much for $\overline{E}\cdot 4^{-2}$ or larger. The deviations shown for smaller emissions perturbations, $\overline{E}\cdot 4^{-3}$ and $\overline{E}\cdot 4^{-4}$, are attributable to numerical noise and round-off error. If the emissions perturbations are too large, visibly nonlinear responses would result, and the social costs could not be considered "marginal." This would be visible in Fig. S1 as a skewing of the results away from 1 for the larger emissions perturbations. For the most part, there is no evidence of that being a problem for the emissions perturbations explored here except some mild deviations for NO_x and NH_3 near the maximum, $\overline{E}\cdot 4^{1}$. For these largest emissions perturbations, social costs for NO_x and NH_3 are slightly but systematically lower than smaller emissions perturbations. This behavior is consistent with known atmospheric chemistry; as the amount of ammonia or nitric acid increases, it is more likely to be stoichiometrically in excess so the marginal effect of adding more is decreased. Intake fractions also showed essentially the same results. We conclude that the size of the emissions perturbations imposed on the model may be considered "marginal" in the sense that they are large enough to avoid spurious numerical noise but small enough not to change the chemical regime appreciably. The results also show that indirect effects outside of our chosen perturbation size (See Section 2.2) do not produce big biases within the wide range of perturbations.

3.2. Description of the generated dataset

Monthly marginal social costs and intake fractions calculated directly using CAMx output for the 100 sample locations are presented in Fig. 2 and S2. When deriving parameterizations, we used social costs and intake fractions calculated for the period of each season as defined in Fig. 2(a). Marginal emissions of NO_x in one rural training location in spring and a remote test location in summer decreased $PM_{2.5}$ concentrations, resulting in negative marginal social costs and intake fractions. Looking at the two samples closely, we determined that they are caused by numerical noise. These two unusual samples were not included when deriving the regression models.

To give a sense of the distributions and correlations of selected variables, correlation matrix plots of selected variables for marginal social cost models are presented in Figs. S3–S6. The maps of meteorological variables we used in parameterizations—temperature, surface atmospheric pressure, absolute precipitation, wind speed, humidity, total sulfate, total nitrate, and total ammonia—are presented in Figs. S7–S14.

3.3. Average plumes

The average plumes are illustrated in Fig. 3 using the summertime results as an example. Fig. S15 shows the complete set of seasonal average plumes. Emissions of all four species have long-range impacts extending over regions larger than 1000 km, but the impacts of SO_2 and NO_x emissions are somewhat wider than EC and NH_3. This is consistent with the fact that SO_2 and NO_x must undergo atmospheric oxidation before $PM_{2.5}$ formation, so their impacts are necessarily more diffuse. Based on these average plume distributions, our method describes the size of exposed population by putting larger weight on population nearby sources and diminishing weights on populations as one moves far from the original source. It is clear from these results that very localized measures of population, such as population density in the source county or grid cell, would fail to describe the exposures resulting from these sources. The population ring method, an alternative method of describing exposed population, is presented and compared in SI.

3.4. Parameterization results

Because we present many regression models (96 in total from 2

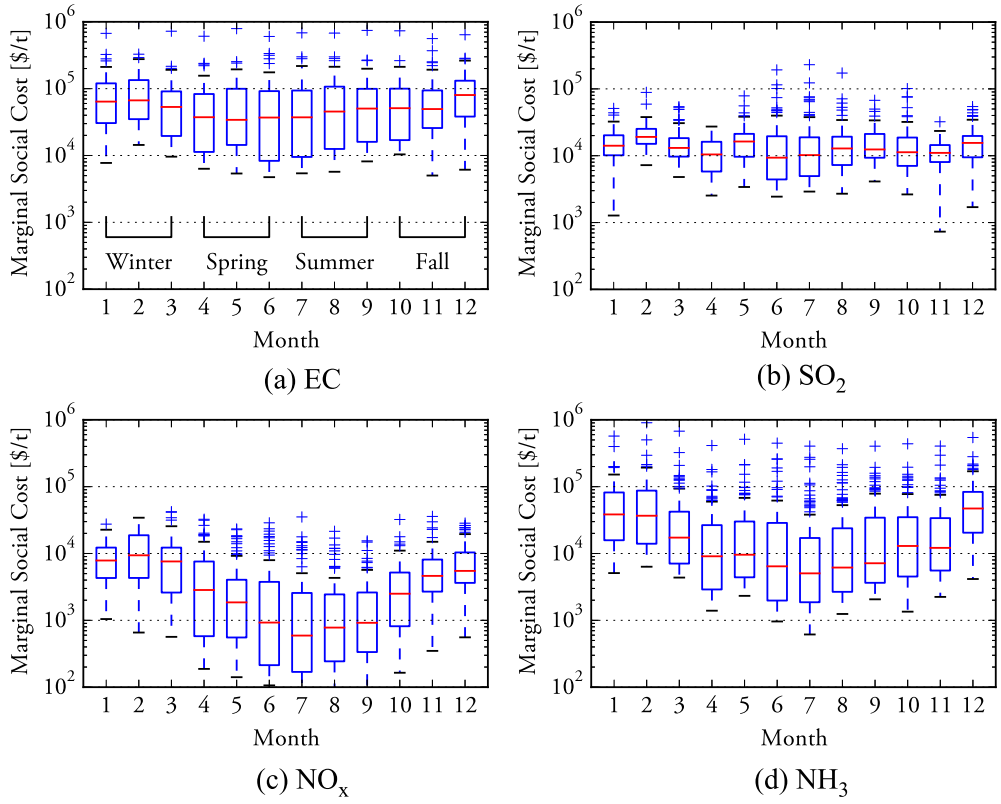

Fig. 2. Marginal social costs at the 100 sample locations. Winter is defined as January to March, spring as April to June, summer as July to September, and fall as October to December. The bottom and top of the box are the first and third quartile, and the red band inside the box indicates median. Whiskers show 1.5 × IQR (interquartile range) below the first quartile and beyond the third quartile. (For interpretation of the references to color in this figure legend, the reader is referred to the web version of this article.)

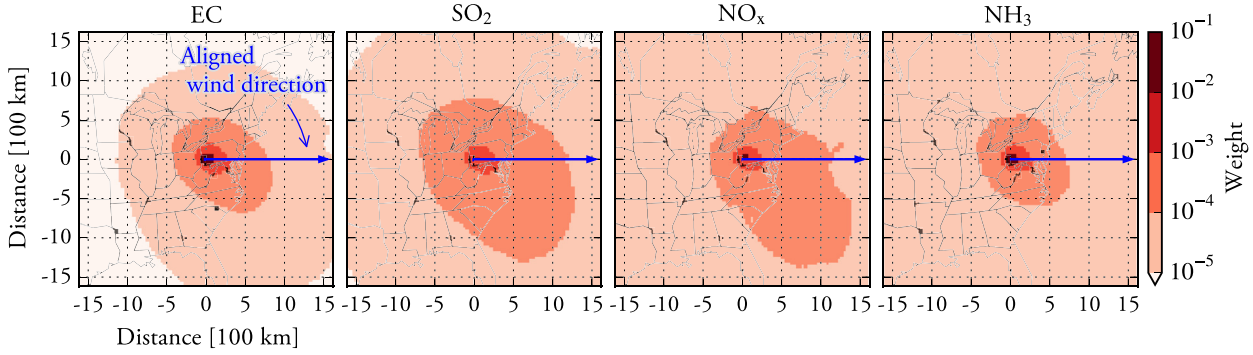

Fig. 3. Average plumes for ground-level emissions in summer. Although the average plume distributions are generic, to illustrate a sense of scale, they are placed on a map with Pittsburgh at the center. Average plumes are skewed to the right from wind direction, which is caused by the rotation of the Earth, or the Coriolis effect.

marginal effects, 4 species, 4 seasons, and 3 emission elevations), we mainly discuss results from marginal social cost models for ground-level emissions, but models for elevated emissions show very similar results. Table 1 presents coefficients and statistics from regressions for marginal social costs in summer. A complete set of results for all seasons and all emission elevations is shown in Tables S1–S3 for marginal social cost and in Tables S4–S6 for intake fraction. Overall, the regression models show a high goodness of fit. The value of adjusted R^2 is 0.9 or higher for most models; 0.7 or higher in fall for SO_2 model, in winter, summer, and fall for NO_x model; and 0.5 for winter SO_2 models. While winter SO_2 models have the lowest adjusted R^2 values, winter SO_2 shows the least variability in social costs (Fig. 2). Prediction intervals for all models are tight; they are within a factor of two except for some NO_x models that are up to a factor of three. A prediction interval measures the expected error between CAMx and EASIUR social costs at a single specific location (e.g. a single model grid cell) whereas the confidence interval would be a measure of uncertainty in predicted social costs when averaged over an ensemble of similar locations.

All the models show good performance from out-of-sample tests. In Fig. 4, estimates with EASIUR are compared to those calculated directly using CTM results for the 50 test samples in summer. The out-of-sample evaluations are summarized in Fig. 5, which is based on the criteria (Morris et al., 2005) using fractional bias and fractional error that evaluates the performance of chemical transport models against measurements. All the seasonal models meet the “excellent” criteria with two exceptions, NO_x models for summer and fall, meeting the “good” criteria. The fractional errors

Table 1
Marginal social cost models for summer season.

	EC	SO_2	NO_x	NH_3
Intercept	83***	74***	230***	−12
	(11)	(14)	(32)	(8.6)
ln (Pop_w)	0.78***	0.56***	0.81**	0.84***
	(0.034)	(0.075)	(0.23)	(0.079)
ln (Temp)	−21***	−20***	−53***	–
	(2.1)	(2.9)	(5.7)	–
ln (Pres)	5.6***	7.3***	9.9***	4.2**
	(0.52)	(0.58)	(1.7)	(1.3)
ln (Humi)	–	−0.74**	–	−1.2***
	–	(0.22)	–	(0.32)
ln (Prec)	–	–	−0.19*	0.24***
	–	–	(0.069)	(0.057)
ln (Wind)	–	–	−0.19	−0.14+
	–	–	(0.13)	(0.076)
ln (TS)	–	0.23+	–	1.1***
	–	(0.13)	–	(0.18)
ln (TN)	–	–	0.43+	−0.30*
	–	–	(0.22)	(0.15)
ln (TA)	–	−0.15***	–	−0.43***
	–	(0.033)	–	(0.059)
Adj. R^2	0.97	0.94	0.86	0.93
F. Bias	−0.0068	0.069	0.076	−0.061
F. Error	0.16	0.23	0.49	0.28
95% PI	[0.66, 1.5]	[0.68, 1.5]	[0.31, 3.2]	[0.49, 2.1]
95% CI	[0.89, 1.1]	[0.86, 1.2]	[0.66, 1.5]	[0.75, 1.3]

***p < 0.001, **p < 0.001, *p < 0.05, +p < 0.1, Standard deviations in parentheses. Pop_w: population (≥ age 30) weighted with average plume [# of people]. Temp: temperature [K]. Pres: surface atmopsheric pressure [hPa]. Humid: humidity [ppm]. Prec: precipitation +0.0002 (shifted for log transformation) [g/m^3]. Wind: wind speed [m/s]. TS: total sulfate (=[SO_4^{2-}]) [μmol/m^3]. TN: total nitrate (=[HNO_3] + [NO_3^-]) [μmol/m^3]. TA: total ammonia (=[NH_3] + [NH_4^+]) [μmol/m^3]. Adj. R^2: adjusted R^2. F. Bias: mean fractional bias. F. Error: mean fractional error. 95% PI: average 95th prediction intervals relative to predicted value. 95% CI: average 95th confidence intervals relative to predicted value.

social costs are lowest in summer, and the NO_x model performs best in winter when NO_x emissions and PM nitrate are most important.

The coefficients of parameters show their role in explaining exposed population and atmospheric processes, although many parameters are correlated and their coefficients do not allow straightforward physical interpretations. The high correlation, it should be noted, is not problematic for us because we are interested in predicting dependent variables (marginal social cost or intake fraction) rather than deriving the unbiased coefficients of explanatory variables. However, correlations do suggest that the regression models developed here for the United States could not be simply translated to other regions. In most models, weighted population, temperature, and atmospheric pressure appeared very significant with p value of 0.001 or less. As expected, weighted population is positively correlated, representing the size of exposed population, which is shown in the correlation matrix plots in Figs. S3–S6. An exception is SO_2 in winter; SO_2 is a long transport species, its photo-oxidation to sulfate $PM_{2.5}$ is weakest, and, therefore, SO_2 social costs are smoothed over the population variability. Temperature is negatively correlated in all models. This likely represents that the higher temperature the higher boundary mixing layer height, which results in more vertical dilution of $PM_{2.5}$, or lower $PM_{2.5}$ concentrations and exposure. Surface atmospheric pressure is positively correlated. The pressure values we used are not sea level adjusted and strongly correlated with surface elevation as can be seen in Fig. S8. This suggests that pressure may be functioning here as a proxy variable for population because population density is low not only in the mountainous areas such as the Rocky Mountains and the Appalachian Mountains but also in the high plateaus such as the Great Basin and the Great Plains while many densely populated urban areas are in coastal or other relatively low-lying areas. The correlation plots confirm that pressure is

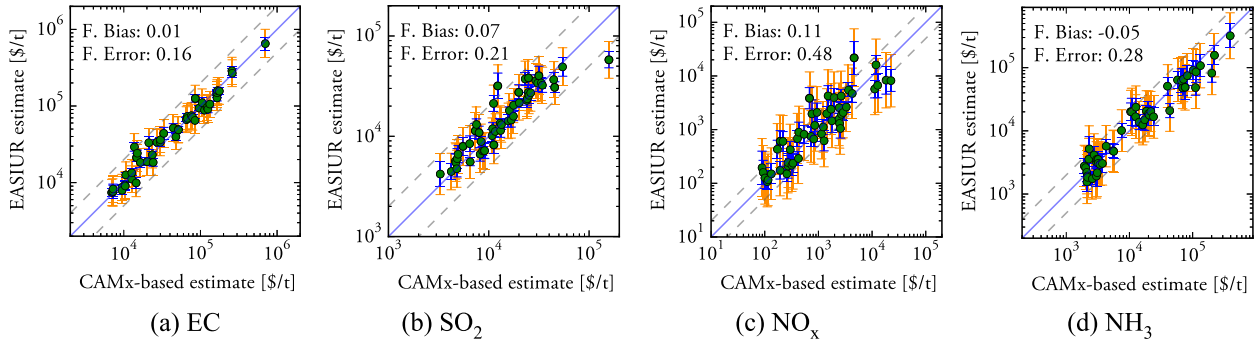

Fig. 4. Out-of-sample evaluations of EASIUR marginal social cost models for summer. Dashed lines indicate a factor of two and solid line indicates unbiased prediction. Orange bars show 95% prediction intervals and blue bars show 95% confidence intervals. Mean fractional bias and mean fractional error are shown at the bottom right corner. (For interpretation of the references to color in this figure legend, the reader is referred to the web version of this article.)

are quite similar in magnitude to the corresponding fractional error metrics between CTMs and observed concentrations of $PM_{2.5}$ species, suggesting that the additional error due to the regression process is acceptable, given the convenience of having a reduced-form model, compared to the error in the full CTM itself. It is also unsurprising that NO_x social costs are the most difficult to parameterize. In $PM_{2.5}$ modeling, it is understood that nitrate is the most difficult component of $PM_{2.5}$ to predict well (Karydis et al., 2007; U.S. EPA, 2011c) as it depends on sulfate and ammonia concentrations as well as nitric acid and also on both gas-phase oxidation and gas-particle partitioning processes. We also stress that the NO_x correlated with weighted population.

Precipitation, wind speed, and humidity appear in many regressions, though they are often not statistically significant. Precipitation generally has negative coefficients, indicating its role in wet deposition, the dominant $PM_{2.5}$ removal mechanism. An exception is summer NH_3 models; this may result from higher humidity favoring the formation of ammonium nitrate PM. Wind speed generally has negative coefficients. Though it may be partly related with the role of wind in dispersion, wind speed is also to be negatively correlated with population density, as shown the consistent negative correlations with population variables in

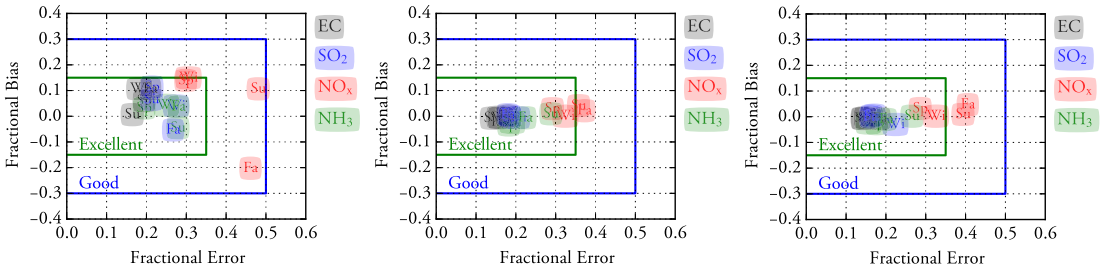

Fig. 5. Cross-validation of marginal social cost models. Wi, Sp, Su, and Fa correspond to winter, spring, summer, and fall, respectively. "Excellent" and "Good" model performance criteria are shown as suggested by Morris et al. (2005). Fractional biases and errors of ground-level models were calculated with the 50 test samples and those of elevated emissions with a five-fold cross-validation method.

correlation plots. Fig. S11 also shows that the windy areas are located along the Rocky Mountains as well as some less-populated parts of the Midwest. Humidity generally has positive coefficients, especially for SO_2 and NO_x in winter and fall. This appears to be related with atmospheric oxidation because there are generally more oxidants like hydroxyl radical when humidity is high.

For inorganic species, total sulfate, total nitrate, and total ammonia are found to be significant parameters in many models. They are highly correlated with each other as well as with weighted population and atmospheric pressure, as shown in the correlation matrix plots. Therefore, the three inorganic parameters may partly describe exposed population. However, it appears that some coefficients represent atmospheric chemistry. TS has negative coefficients in SO_2 and NO_x models in winter and fall seasons, when atmospheric oxidants are limited than other seasons. The higher TS may indicate the limited availability of atmospheric oxidants for SO_2 or NO_x oxidation. For NO_x models in winter and fall, TS may additionally represent the phase partitioning thermodynamics of $PM_{2.5}$ (Ansari and Pandis, 1998). The higher TS would limit NO_x to form PM nitrate formation in cold seasons.

3.5. The length of CTM simulation period

Although we simulated a whole-year period, it is useful to know the length of CTM simulation required to achieve a seasonal average given that the CTM simulations are computationally expensive. In Fig. 6, marginal social costs calculated using periods of two weeks, four weeks, and eight weeks in the middle of each season were compared to those using the entire season period. More detailed boxplots are presented in Fig. S17. According to the results, a two-week period is sufficient for EC to represent its corresponding season because it falls in "excellent" range compared to entire season periods. For other secondary species, a two- or four-week period generally appears sufficient ("excellent" or "good" compared to entire seasons) except Fall NH_3. Fall NH_3 showed relatively large biases and errors because short mid-season periods of the fall season form much less nitrate ammonium PM than the end of the season (December), which can be seen in Fig. 2(d). This result will be useful for further reducing computational burden associated with EASIUR development and evaluation in the future.

3.6. Adjusting EASIUR estimates for important parameters

Though EASIUR models assume reasonable fixed values for several important parameters associated with relative risk, population, baseline mortality rate, dollar year and income level for VSL, and $PM_{2.5}$ mortality lag structure, it is often necessary to use different values for these parameters. Doing so will be useful not only for producing estimates with different values for these parameters, but also for uncertainty analysis associated with these factors. We discussed each parameter in detail and presented simple methods for adjusting for these parameters in SI.

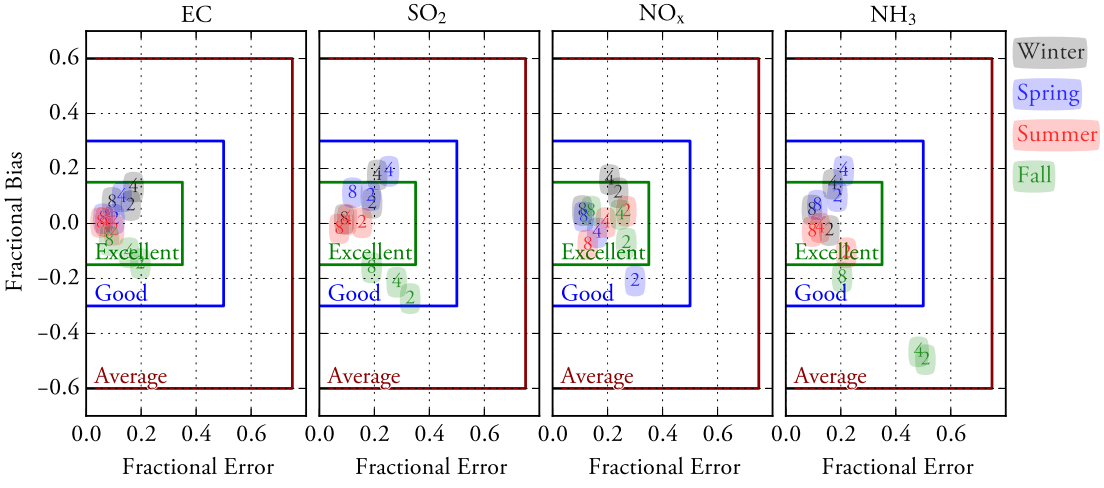

Fig. 6. Fractional error and bias of marginal social costs using different simulation periods against the full seasonal periods. In order to explore the length of simulation period that can represent a season, marginal social costs calculated using periods of two weeks, four weeks, and eight weeks are compared to those using a full season period. The number at each point indicates the simulation period in week. "Excellent," "Good," and "Average" criteria from Morris et al. (2005) are shown as reference.

4. Conclusions

We developed the Estimating Air pollution Impact Using Regression (EASIUR) model, which estimates the social cost of emissions like a state-of-the-art chemical transport model but without high computational costs. Our method employed a CTM so that our results are consistent with up-to-date atmospheric science. This is the first time that a set of CTM-derived impact metrics are presented for use in policy assessments with high spatial resolution (36 km or approximately county scale) according to source location.

Accomplishing this objective required efficient means to address several challenges. Tagged simulations allowed us to create computationally efficiently a large dataset of marginal public health costs and intake fractions for a carefully chosen size of "marginal" emissions at 100 random locations in the U.S. In order to describe population exposure occurring at large downwind areas, we developed the average plume method and the population ring method. We chose the average plume method because it generally worked better. Finally, regression models were built to parameterize marginal social cost and intake fraction with exposed population and key atmospheric variables. Fractional errors of the models' estimates of marginal social cost and intake fraction against the computationally expensive CTM-based estimates are mostly 10–30% and up to ~50% for some NO_x models, which is comparable to or less than those of CTM outputs against measurement. Considering CTM's uncertainty, our method, therefore, would estimate the public health effects without adding large uncertainties from air quality modeling. We also found that about 2–4 week simulation periods will be able to represent a season for elemental carbon and inorganic gases so that the CTM may not need to be run for the entire season period.

In this paper, we focused on developing and evaluating the methods for deriving the EASIUR model of four species (EC, SO_2, NO_x, and NH_3) for four seasons and for three elevation heights. The EASIUR model results are currently provided in the Internet: <http://barney.ce.cmu.edu/~jinhyok/easiur/>. In a separate paper (Heo et al., 2016), we present marginal social costs and intake fractions estimated by the EASIUR model for across the United States, detailed discussion of uncertainties, and comprehensive comparisons to other studies. We also plan to derive EASIUR based on the 2014 National Emissions Inventory (U.S. EPA, 2015b) in near future.

Acknowledgments

The authors thank Bonyoung Koo and Ben Murphy for valuable advice for CTM simulations. This work was supported by the center for Climate and Energy Decision Making (SES-0949710), through a cooperative agreement between the National Science Foundation and Carnegie Mellon University.

Appendix A. Supplementary data

Supplementary data related to this article can be found at http://dx.doi.org/10.1016/j.atmosenv.2016.04.026.

References

Akaike, H., 1974. A new look at the statistical model identification. IEEE Trans. Autom. Control 19, 716–723. http://dx.doi.org/10.1109/TAC.1974.1100705.

Ansari, A.S., Pandis, S.N., 1998. Response of inorganic PM to precursor concentrations. Environ. Sci. Technol. 32, 2706–2714. http://dx.doi.org/10.1021/es971130j.

Arunachalam, S., Wang, B., Davis, N., Baek, B.H., Levy, J.I., 2011. Effect of chemistry-transport model scale and resolution on population exposure to $PM_{2.5}$ from aircraft emissions during landing and takeoff. Atmos. Environ. 45, 3294–3300. http://dx.doi.org/10.1016/j.atmosenv.2011.03.029.

Bennett, D.H., McKone, T.E., Evans, J.S., Nazaroff, W.W., Margni, M.D., Jolliet, O., Smith, K.R., 2002. Defining intake fraction. Environ. Sci. Technol. 36, 206A–211A. http://dx.doi.org/10.1021/es0222770.

Buonocore, J.J., Dong, X., Spengler, J.D., Fu, J.S., Levy, J.I., 2014. Using the community multiscale air quality (CMAQ) model to estimate public health impacts of $PM_{2.5}$ from individual power plants. Environ. Int. 68, 200–208. http://dx.doi.org/10.1016/j.envint.2014.03.031.

Byun, D., Schere, K.L., 2006. Review of the governing equations, computational algorithms, and other components of the models-3 community multiscale air quality (CMAQ) modeling system. Appl. Mech. Rev. 59, 51–77. http://dx.doi.org/10.1115/1.2128636.

Dunker, A.M., Yarwood, G., Ortmann, J.P., Wilson, G.M., 2002. The decoupled direct method for sensitivity analysis in a three-dimensional air quality model implementation, accuracy, and efficiency. Environ. Sci. Technol. 36, 2965–2976. http://dx.doi.org/10.1021/es0112691.

ENVIRON, 2012. CAMx User's Guide Version 5.41. Environ International Corporation, Novato, CA.

Fann, N., Baker, K.R., Fulcher, C.M., 2012. Characterizing the $PM_{2.5}$-related health benefits of emission reductions for 17 industrial, area and mobile emission sectors across the U.S. Environ. Int. 49, 141–151. http://dx.doi.org/10.1016/j.envint.2012.08.017.

Fann, N., Fulcher, C.M., Hubbell, B.J., 2009. The influence of location, source, and emission type in estimates of the human health benefits of reducing a ton of air pollution. Air Qual. Atmos. Health 2, 169–176. http://dx.doi.org/10.1007/s11869-009-0044-0.

Grell, G.A., Dudhia, J., Stauffer, D.R., 1994. A Description of the Fifth-Generation Penn State/NCAR Mesoscale Model (MM5). NCAR Technical Note NCAR/TN-398 + STR. http://dx.doi.org/10.5065/D60Z716B.

Hakami, A., Henze, D.K., Seinfeld, J.H., Singh, K., Sandu, A., Kim, S., Byun, Li, Q., 2007. The adjoint of CMAQ. Environ. Sci. Technol. 41, 7807–7817. http://dx.doi.org/10.1021/es070944p.

Henze, D.K., Hakami, A., Seinfeld, J.H., 2007. Development of the adjoint of GEOS-chem. Atmos. Chem. Phys. 7, 2413–2433. http://dx.doi.org/10.5194/acp-7-2413-2007.

Heo, J., Adams, P.J., Gao, H.O., 2016. Public health costs of primary $PM_{2.5}$ and inorganic $PM_{2.5}$ precursor emissions in the United States. Manuscript submitted for publication.

Hubbell, B.J., Hallberg, A., McCubbin, D.R., Post, E., 2005. Health-related benefits of attaining the 8-Hr ozone standard. Environ. Health Perspect. 113, 73–82. http://dx.doi.org/10.1289/ehp.7186.

Karydis, V.A., Tsimpidi, A.P., Pandis, S.N., 2007. Evaluation of a three-dimensional chemical transport model (PMCAMx) in the eastern United States for all four seasons. J. Geophys. Res. 112, D14211. http://dx.doi.org/10.1029/2006JD007890.

Koo, B., Dunker, A.M., Yarwood, G., 2007. Implementing the decoupled direct method for sensitivity analysis in a particulate matter air quality model. Environ. Sci. Technol. 41, 2847–2854. http://dx.doi.org/10.1021/es0619962.

Koo, B., Wilson, G.M., Morris, R.E., Dunker, A.M., Yarwood, G., 2009. Comparison of source apportionment and sensitivity analysis in a particulate matter air quality model. Environ. Sci. Technol. 43, 6669–6675.

Krewski, D., Burnett, R.T., Goldberg, M.S., Hoover, B.K., Siemiatycki, J., Jerrett, M., Abrahamowicz, M., White, W.H., 2003. Overview of the reanalysis of the Harvard six cities study and American cancer society study of particulate air pollution and mortality. J. Toxicol. Environ. Health A 66, 1507–1551. http://dx.doi.org/10.1080/15287390306424.

Krewski, et al., 2009. Extended Follow-up and Spatial Analysis of the American Cancer Society Study Linking Particulate Air Pollution and Mortality. Health Effects Institute, Boston, MA (Research Report 140).

Kwok, R.H.F., Baker, K.R., Napelenok, S.L., Tonnesen, G.S., 2015. Photochemical grid model implementation and application of VOC, NO_x, and O_3 source apportionment. Geosci. Model Dev. 8, 99–114. http://dx.doi.org/10.5194/gmd-8-99-2015.

Latimer, D.A., 1996. Particulate Matter Source-receptor Relationships between All Point and Area Sources in the United States and PSD Class I Area Receptors (VI-A-2 A-95–83) (Prepared for U.S. EPA, OAQPS, Research Triangle Park, NC).

Lelieveld, J., Evans, J.S., Fnais, M., Giannadaki, D., Pozzer, A., 2015. The contribution of outdoor air pollution sources to premature mortality on a global scale. Nature 525, 367–371. http://dx.doi.org/10.1038/nature15371.

Lepeule, J., Laden, F., Dockery, D., Schwartz, J., 2012. Chronic exposure to fine particles and mortality: an extended follow-up of the Harvard six cities study from 1974 to 2009. Environ. Health Perspect. 120, 965–970. http://dx.doi.org/10.1289/ehp.1104660.

Levy, J.I., Baxter, L.K., Schwartz, J., 2009. Uncertainty and variability in health-related damages from coal-fired power plants in the United States. Risk Anal. 29, 1000–1014. http://dx.doi.org/10.1111/j.1539-6924.2009.01227.x.

Lim, et al., 2012. A comparative risk assessment of burden of disease and injury attributable to 67 risk factors and risk factor clusters in 21 regions, 1990–2010: a systematic analysis for the global burden of disease study 2010. Lancet 380, 2224–2260. http://dx.doi.org/10.1016/S0140-6736(12)61766-8.

Morris, R.E., McNally, D.E., Tesche, T.W., Tonnesen, G., Boylan, J.W., Brewer, P., 2005. Preliminary evaluation of the community multiscale air quality model for 2002 over the southeastern United States. J. Air Waste Manag. Assoc. 55, 1694–1708.

Muller, N.Z., 2011. Linking policy to statistical uncertainty in air pollution damages. BE J. Econ. Anal. Policy 11. http://dx.doi.org/10.2202/1935-1682.2925,

1935–1682.
Muller, N.Z., Mendelsohn, R., 2009. Efficient pollution regulation: getting the prices right. Am. Econ. Rev. 99, 1714–1739. http://dx.doi.org/10.1257/aer.99.5.1714.
National Research Council, 2010. Hidden Costs of Energy: Unpriced Consequences of Energy Production and Use. The National Academies Press, Washington, DC.
Pinder, R.W., Dennis, R.L., Bhave, P.V., 2008. Observable indicators of the sensitivity of $PM_{2.5}$ nitrate to emission reductions–part I: derivation of the adjusted gas ratio and applicability at regulatory-relevant time scales. Atmos. Environ. 42, 1275–1286. http://dx.doi.org/10.1016/j.atmosenv.2007.10.039.
Pope III, C.A., Dockery, D.W., 2006. Health effects of fine particulate air pollution: lines that connect. J. Air Waste Manag. Assoc. 56, 709–742.
Punger, E.M., West, J.J., 2013. The effect of grid resolution on estimates of the burden of ozone and fine particulate matter on premature mortality in the USA. Air Qual. Atmos. Health 6, 563–573. http://dx.doi.org/10.1007/s11869-013-0197-8.
Robinson, A.L., Donahue, N.M., Shrivastava, M.K., Weitkamp, E.A., Sage, A.M., Grieshop, A.P., Lane, T.E., Pierce, J.R., Pandis, S.N., 2007. Rethinking organic aerosols: semivolatile emissions and photochemical aging. Science 315, 1259–1262. http://dx.doi.org/10.1126/science.1133061.
Thompson, T.M., Saari, R.K., Selin, N.E., 2014. Air quality resolution for health impact assessment: influence of regional characteristics. Atmos. Chem. Phys. 14, 969–978. http://dx.doi.org/10.5194/acp-14-969-2014.
US Burden of Disease Collaborators, 2013. The state of US health, 1990–2010: burden of diseases, injuries, and risk factors. JAMA 310, 591–606. http://dx.doi.org/10.1001/jama.2013.13805.
U.S. EPA, 2015a. Environmental Benefits Mapping and Analysis Program – Community Edition (BenMAP-CE) Version 1.1. U.S. Environmental Protection Agency., Research Triangle Park, NC. http://www2.epa.gov/benmap/.
U.S. EPA, 2015b. 2011 National Emissions Inventory. http://www.epa.gov/air-emissions-inventories/national-emissions-inventory (accessed Nov 1, 2015).
U.S. EPA, 2014. Regulatory Impact Analysis for the Proposed Carbon Pollution Guidelines for Existing Power Plants and Emission Standards for Modified and Reconstructed Power Plants (EPA-452/R-14-002). U.S. Environmental Protection Agency. Office of Air Quality Planning and Standards. Health & Environmental Impacts Division. Air Economics Group, Research Triangle Park, NC.
U.S. EPA, 2013. User's Manual for the Co-benefits Risk Assessment (COBRA) Screening Model Version: 2.61. U.S. Environmental Protection Agency, Washington, DC.
U.S. EPA, 2011a. The Benefits and Costs of the Clean Air Act from 1990 to 2020. U.S. Environmental Protection Agency. Office of Air and Radiation, Washington, DC.
U.S. EPA, 2011b. Regulatory Impact Analysis for the Federal Implementation Plans to Reduce Interstate Transport of Fine Particulate Matter and Ozone in 27 States; Correction of SIP Approvals for 22 States (EPA-HQ-OAR-2009-0491). U.S. Environmental Protection Agency, Office of Air and Radiation.
U.S. EPA, 2011c. Air Quality Modeling Final Rule Technical Support Document. U.S. Environmental Protection Agency. Office of Air Quality Planning and Standards. Air Quality Assessment Division.
U.S. EPA, 2011d. Emissions Inventory Final Rule TSD (EPA-HQ-OAR-2009-0491). U.S. Environmental Protection Agency. Office of Air and Radiation. Office of Air Quality Planning and Standards. Air Quality Assessment Division.
U.S. EPA, 2006. Technical Support Document for the Proposed PM NAAQS Rule, Response Surface Modeling. Office of Air Quality Planning and Standards, Research Triangle Park, NC.
U.S. EPA, 1999. The Benefits and Costs of the Clean Air Act, 1990 to 2010, EPA Report to Congress (EPA-410-R-99–001). U.S. Environmental Protection Agency. Office of Air and Radiation. Office of Policy, Washington, DC.
Wagstrom, K.M., Pandis, S.N., Yarwood, G., Wilson, G.M., Morris, R.E., 2008. Development and application of a computationally efficient particulate matter apportionment algorithm in a three-dimensional chemical transport model. Atmos. Environ. 42, 5650–5659. http://dx.doi.org/10.1016/j.atmosenv.2008.03.012.
West, J.J., Ansari, A.S., Pandis, S.N., 1999. Marginal $PM_{2.5}$: nonlinear aerosol mass response to sulfate reductions in the eastern United States. J. Air Waste Manag. Assoc. 49, 1415–1424.